Protein Thermal Aggregation Involves Distinct Regions: Sequential Events in the Heat-Induced Unfolding and Aggregation of Hemoglobin

Yong-Bin Yan,*† Qi Wang,* Hua-Wei He,* and Hai-Meng Zhou*‡
*Department of Biological Sciences and Biotechnology, †State Key Laboratory of Biomembrane and Membrane Biotechnology, and ‡Protein Science Laboratory of the Ministry of Education, Tsinghua University, Beijing 100084, China

ABSTRACT Protein thermal aggregation plays a crucial role in protein science and engineering. Despite its biological importance, little is known about the mechanism and pathway(s) involved in the formation of aggregates. In this report, the sequential events occurring during thermal unfolding and aggregation process of hemoglobin were studied by two-dimensional infrared correlation spectroscopy. Analysis of the infrared spectra recorded at different temperatures suggested that hemoglobin denatured by a two-stage thermal transition. At the initial structural perturbation stage (30–44°C), the fast red shift of the band from α-helix indicated that the native helical structures became more and more solvent-exposed as temperature increased. At the thermal unfolding stage (44–54°C), the unfolding of solvent-exposed helical structures dominated the transition and was supposed to be responsible to the start of aggregation. At the thermal aggregation stage (54–70°C), the transition was dominated by the formation of aggregates and the further unfolding of the buried structures. A close inspection of the sequential events occurring at different stages suggested that protein thermal aggregation involves distinct regions.

INTRODUCTION

Self-association in a controlled manner to generate functional complexes is an important feature of a variety of biological processes (Schreiber, 2002). However, uncontrolled aggregation of proteins has been associated with a series of diseases, including sickle-cell anemia disease, Alzheimer's disease, Parkinson's disease, and Huntington's disease (Noguchi and Schechter, 1985; Carrell and Gooptut, 1998; Hoffner and Djian, 2002). Protein aggregation is also a common feature in protein engineering, and the refolding procedure is a problem of significant economic importance (Kopito, 2000). Despite its biological importance, neither the assemble mechanism nor the atomic structures of the aggregates are known (Thirumalai et al., 2003). To study the mechanism and pathways involved in aggregation, the probes that are used are important and should be sensitive enough to detect the closely related events. Normal probes used in protein folding studies, such as circular dichroism, fluorescence, and NMR, are difficult to follow the aggregation process because these techniques are sensitive to light scattering (Dong et al., 2000). Infrared (IR) spectroscopy is insensitive to light scattering and thus has been widely used in protein folding and aggregation studies (Jackson et al., 1989). With the development of two-dimensional infrared (2D IR) correlation spectroscopy in recent years (Noda, 1989, 1990, 1993), IR spectroscopy has become a powerful tool to characterize the native secondary structure elements (Nabet and Pézolet, 1997) and to investigate the closely related events occurring in the protein folding and aggregation processes (for example, Fabian et al., 1999; Filosa et al., 2001; Paquet et al., 2001; Yan et al., 2003).

The thermal aggregation of proteins is usually characterized as an irreversible two-state model (Lyubarev, 1999; Dong et al., 2000). However, the occurrence of folding/unfolding intermediate or uncooperative event(s) has been observed by several studies (Bulone et al., 2001; Filosa et al., 2001; Paquet et al., 2001; Yan et al., 2002, 2003). The intermediate and uncooperative events observed might be important to protein folding and aggregate formation (Carrotta et al., 2001; Yan et al., 2002; Srisailam et al., 2003). Thermal aggregation was also found to occur between nearly native proteins under certain conditions (Tsai et al., 1998; Paquet et al., 2001; Yan et al., 2003). These findings argued that the start of thermal aggregation might not require fully unfolded proteins, but rather some necessary regions for the formation of intermolecular interactions. Such a hypothesis has been verified in the study of amyloid fibrils formation (Chiti et al., 2002), but has not been characterized in the thermal aggregation studies.

In this study, the sequential events in hemoglobin (Hb) thermal transitions were monitored by IR spectroscopy. To obtain detailed information related to unfolding and aggregation, 2D IR correlation plots were constructed at small-step perturbations (every 10°C intervals) in addition to full temperature range. A two-step thermal transition was observed and the order of the related events was analyzed by 2D IR correlation. It is interesting that different vibration patterns of the same secondary structure could be identified by the asynchronous plots. Two classes of intensities, which were related to different events, were clearly distinguished at the beginning stage of thermal aggregation. These findings suggested that the evolution of thermal aggregation was a quite complex process involving lots of noncooperative events. The method of 2D IR correlation spectroscopy pro-

Submitted August 25, 2003, and accepted for publication October 7, 2003.

Address reprint requests to Dr. Yong-Bin Yan, NMR Laboratory, Dept. of Biological Sciences and Biotechnology, Tsinghua University, Beijing 100084, China. Tel.: +86-10-6278-3477; Fax: +86-10-6277-1597; E-mail: ybyan@mail.tsinghua.edu.cn.

© 2004 by the Biophysical Society

0006-3495/04/03/1682/09 $2.00

vides a powerful tool to detect the evolution and order of these minor changes.

MATERIALS AND METHODS

Infrared measurements

Bovine hemoglobin was purchased from Sigma Chemical (St. Louis, MO) and used without further purification. Details regarding the sample preparation and the recording of IR spectra were the same as those described before (Yan et al., 2003). In brief, IR experiments were carried out with a 50 mg/ml Hb solution (pD 7.8) after H/D exchange was completed. Infrared spectra were measured at a spectral resolution of 4 cm^{-1} in a single-beam mode with a PerkinElmer (Wellesley, MA) Spectrum 2000 spectrometer equipped with a dTGS detector. Protein samples were placed between a pair of CaF_2 windows separated by a 50-μm Teflon spacer. Spectra were collected in the temperature range of 30–70°C at intervals of 2°C every 20 min. For each measurement, 256 scans were recorded for better signal/noise ratio. The resultant spectra were obtained by subtracting the reference spectra of D_2O from the spectra of the protein solutions. The final unsmoothed spectra were used for further analysis. Spectra recorded above 70°C were similar to that recorded at 70°C and were not included in this research.

2D correlation analysis

Synchronous and asynchronous correlation intensities were computed for the IR spectra at different temperatures by applying the generalized 2D correlation algorithm of Noda (1993). 2D IR correlation plots of different temperature range were constructed with a calculated spectral region of 1700–1600 cm^{-1}. Software (SDIApp) used for calculation was developed in-house according to the generalized 2D correlation algorithm based on the Hilbert transform. Rules used for the analysis of the sign of the peaks in the 2D IR correlation plots were followed by those proposed by Noda (1990, 1993).

RESULTS AND DISCUSSION

Thermal unfolding of Hb from one-dimensional FTIR spectroscopy

The Fourier transform infrared (FTIR) spectra in the amide I region, 1600–1700 cm^{-1}, of Hb solutions heated from 30 to 70°C, are shown in Fig. 1 *A*. At temperatures below 60°C, the amide I region was dominated by the α-helix band at 1651 cm^{-1}. The original FTIR spectra showed that the absorbance of the amide I band kept almost unchanged when the temperature was below 44°C (tentatively called the initiate perturbation stage), and then the intensity of 1651 cm^{-1} gradually decreased at temperatures above 44°C. Two new bands at 1681 (weak) and 1618 cm^{-1} (strong), which has been previously assigned to hydrogen-bonded extended intermolecular β-sheet structures formed upon aggregation of thermally denatured proteins (Damaschun et al., 2000), was observed above 60°C. The thermal denaturation curve of Hb obtained by measuring the intensity at 1651 cm^{-1} showed a distinct three-state model (Fig. 1 *B*). The denaturation of native α-helix (band 1651 cm^{-1}) in Hb could be described by a model involving two consecutive irreversible steps, in which a partial unfolding step (tentatively called the unfolding stage) is followed by an irreversible unfolding step (the aggregation stage) indicated by the intensity increase at 1618 cm^{-1} and 1681 cm^{-1}. According to the classical Lumry and Eyring model (1954), the heat-induced denaturation of Hb was assumed to proceed according to the scheme $N \leftrightarrow U \rightarrow D$, where N, U, and D are the native, unfolded or partially unfolded, and denatured (in our case, aggregation) states, respectively. The midpoint for the unfolding stage was 48°C and that for the aggregation stage was above 62°C.

2D IR correlation analysis

The methodology of 2D IR correlation spectroscopy could be applied to establish band correlations between unfolding and aggregation. Fig. 2 shows two correlation plots, the synchronous and asynchronous spectra, generated from 21 IR spectra of Hb recorded at different temperatures (30–70°C) with a calculated spectral region of 1700–1600 cm^{-1}. In general, the synchronous spectrum is characterized by autopeaks located on the diagonal and by crosspeaks that are off-diagonally placed, whereas asynchronous 2D correlation is characterized by asymmetric crosspeaks and should be more valuable since spectral intensities varying slightly out of phase could be distinguished. The crosspeak may have either positive or negative intensities in both synchronous and asynchronous plots. The crosspeaks in the synchronous plot reflect that correlated events occur simultaneously and the sign indicates the correlated events vary in the same or opposite direction. The crosspeaks in the asynchronous plot only develop when their intensities vary out of phase with

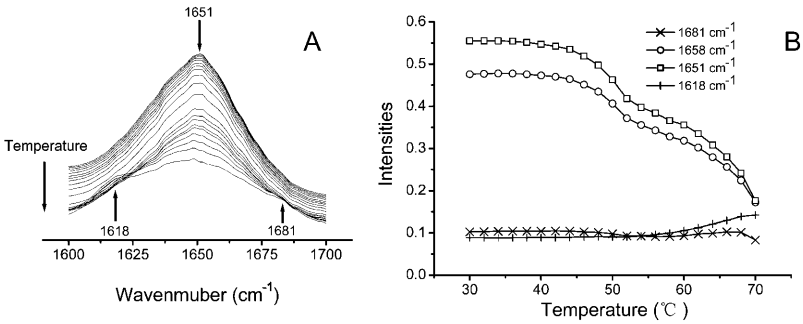

FIGURE 1 Original IR spectra (*A*) and the thermodynamic plot (*B*) of hemoglobin as a function of temperature from 30 to 70°C. The thermodynamic curve was represented by intensity versus temperature plot of the band at 1651 (○) and 1658 cm^{-1} (□), reflecting the unfolding of the native helical structure, and of the band at 1618 (+) and 1681 cm^{-1} (×), reflecting the formation of intermolecular β-sheets.

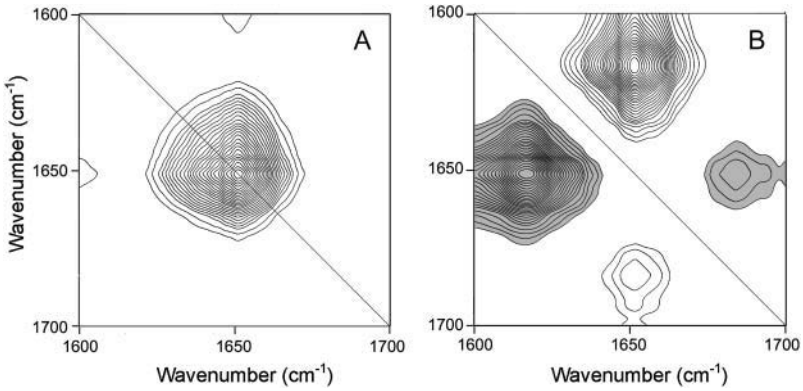

FIGURE 2 Synchronous (*A*) and asynchronous (*B*) 2D IR correlation plots constructed from the 21 spectra recorded at 2°C intervals during Hb thermal transition from 30 to 70°C. Clear and dark peaks are positive and negative, respectively.

each other, and combined analysis of the sign in the synchronous and asynchronous plot could give information about the sequence of events (Noda, 1990, 1993). The synchronous spectrum of Hb in Fig. 2 *A* was dominated by a prominent autopeak at 1651 cm^{-1}, which identified change that occurs in the secondary structure of the protein during the processes of thermal unfolding was dominated by the unfolding of native α-helix. No crosspeaks could be identified in the synchronous plot. Two asymmetric crosspeaks in the amide I region (weak peak at 1651-1684 and strong peak at 1651-1617 cm^{-1}) were observed in the asynchronous spectrum (Fig. 2 *B*), suggesting that the unfolding of native α-helix was followed by the formation of intermolecular β-sheet structures. These results were consisted to those from Fig. 1, and no more new information could be obtained from Fig. 2. It is imaginable that the minor changes in secondary structures might be insidious under the dominant changes of native α-helix and intermolecular β-sheet structures. To solve this problem, 2D correlation was constructed from temperature variations of 30–44°C (the initial perturbation stage), 44–54°C (the unfolding stage), and 54–68°C (the aggregation stage). The assignment of the peaks in the 2D IR analysis was referenced to the previous works (Byler and Susi, 1986; Jackson, 1989; Dong et al., 1990; Dong and Caughey, 1994; Haris and Chapman, 1995; Damaschun et al., 2000) and summarized in Table 1.

Structural perturbations at low temperatures from 30 to 44°C

Fig. 3 shows the synchronous and asynchronous 2D IR correlation plots of Hb thermal transitions generated from FTIR spectra recorded at different temperatures from 30 to 44°C. The traditional one-dimensional (1D) FTIR analysis revealed no significant conformational changes occurred in this temperature range. However, the prominent autopeaks on the diagonal at 1634 and 1653 cm^{-1} in the synchronous plot of Hb (Fig. 3 *A*) suggested that distinct conformational changes already occurred in this temperature region. The band between 1630 and 1640 cm^{-1} is generally assigned to the β-sheet (Jackson, 1989; Nabet and Pézolet, 1997). However, no β-sheet structure existed in the native protein, and the band at 1634 cm^{-1} should be assigned to the hydrogen-bonded extended chains that connect the helical cylinders (Byler and Susi, 1986; Yan et al., 2003). All bands involving amide I presented positive crosspeaks in the synchronous plot and the dominant crosspeaks were found to correlate to the band at 1653 cm^{-1} and 1634 cm^{-1}. Weak autopeaks could be found at 1674, 1681, and 1694 cm^{-1}, which should be assigned to β-turns (Byler and Susi, 1986). More detailed information involving the sequential changes of the protein could be obtained from the asynchronous 2D correlation plots in Fig. 3 *B*. Generally, in protein-folding studies, the appearance of asynchronous crosspeaks allows

TABLE 1 Correlation between the secondary structures and the amide I frequencies observed in the 2D IR correlation plots at different stages of hemoglobin thermal transitions

	Initial perturbation stage (30–44°C)		Thermal unfolding stage (44–54°C)		Thermal aggregation stage (54–70°C)	
Assignment (secondary structure)	Synchronous (cm^{-1})	Asynchronous (cm^{-1})	Synchronous (cm^{-1})	Asynchronous (cm^{-1})	Synchronous (cm^{-1})	Asynchronous (cm^{-1})
Side chains		1615				
Extended chains	1634	1622, 1629, 1634		1634, 1638		
Random coil		1648		1644, 1648		
α-helix	1653	1653, 1657	1651	1652, 1655	1652	1652
3_{10}-helix				1661, 1666		
β-turn	1674, 1681, 1694	1668, 1671, 1676, 1684		1674, 1692		
Intermolecular β-sheet				1618, 1681	1616	1616, 1682

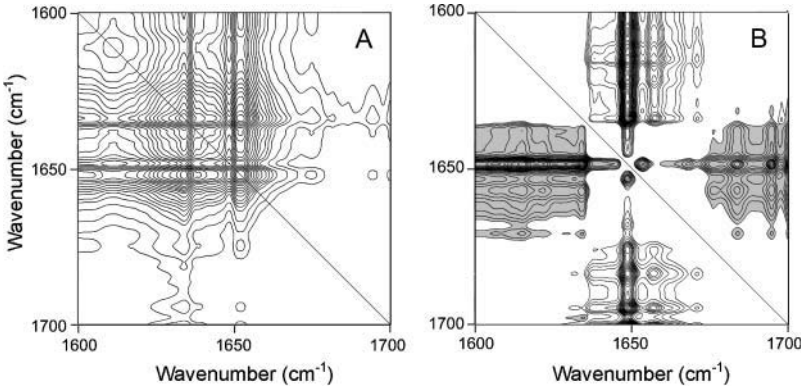

FIGURE 3 Two-dimensional correlation analysis of the IR spectra of Hb at the initial structural perturbation stage. Synchronous (*A*) and asynchronous (*B*) plots were constructed from the eight spectra recorded at temperatures increasing from 30 to 44°C. Clear and dark peaks are positive and negative, respectively.

the detection of differences in the stability of different secondary structure elements. In Fig. 3 *B*, asynchronous crosspeaks could be found between every secondary structure elements and thus allowed to identify the different stability when the protein was suffered to minor temperature perturbations. Numerous new bands appeared in Fig. 3 *B* and located at 1615, 1622, 1629, 1648, 1657, 1668, 1671, 1676, and 1684 cm^{-1}. Similar to the assignment of the band at 1634 cm^{-1}, the band at 1622 and 1629 cm^{-1} should also be assigned to hydrogen-bonded extended chains that connect the helical cylinders (Byler and Susi, 1986; Yan et al., 2003). The band at 1615 cm^{-1} was assigned to extended side chains, whereas the band at 1668, 1671, 1676, and 1684 cm^{-1} was assigned to β-turns. It is interesting that two distinct wavenumber positions (at 1653 and 1657 cm^{-1}), both corresponding to α-helix, are observed and no crosspeaks formed between these two intensities, suggesting that the native α-helix structure in Hb could be characterized by two spectral features that were associated with slightly different strengths of hydrogen bonding of the C=O group. This phenomenon was also observed in other proteins, such as myoglobin (Yan et al., 2003) and ribonuclease A (Schultz et al., 1998). The change of the component at 1653 cm^{-1} was more significant than the component at 1657 cm^{-1} in this temperature range, as characterized by the synchronous autopeak in Fig. 3 *A*. The strongest crosspeaks in Fig. 3 *B* was found correlating 1648 cm^{-1} and other intensities, and the sign indicated that the change of random coil was earlier than all other structural components. The other crosspeaks were found to correlate the band at 1657 cm^{-1} from α-helix and the band at 1671 cm^{-1} from β-turn with all other secondary structure elements. The sign of these crosspeaks suggested that the changes of random coil at 1648 cm^{-1}, α-helix at 1657 cm^{-1}, and β-turn at 1671 cm^{-1} were earlier than the changes of other secondary structure elements. The sequential events during this temperature range could be identified from the signs in the asynchronous plot and are summarized here: random coil (1648 cm^{-1}), α-helix (1657 cm^{-1}), β-turn (1671 cm^{-1}) $\rightarrow$ extended chains (1622, 1629, 1634 cm^{-1}) $\rightarrow$ side chain (1615 cm^{-1}); random coil (1648 cm^{-1}), α-helix (1657 cm^{-1}), β-turn (1671 cm^{-1}) $\rightarrow$ β-turns (1668, 1676, 1684, and 1694 cm^{-1}); random coil (1648 cm^{-1}) $\rightarrow$ α-helix (1653 cm^{-1}).

Thermal unfolding process of Hb from 44 to 54°C

During the temperature interval from 44 to 54°C, significant unfolding of the native structures could be identified from the traditional 1D IR analysis. Different from the initiate structural perturbation stage from 30 to 44°C, only one major autopeak at 1651 cm^{-1} was observed in the synchronous 2D correlation plot in Fig. 4 *A*. This suggested that

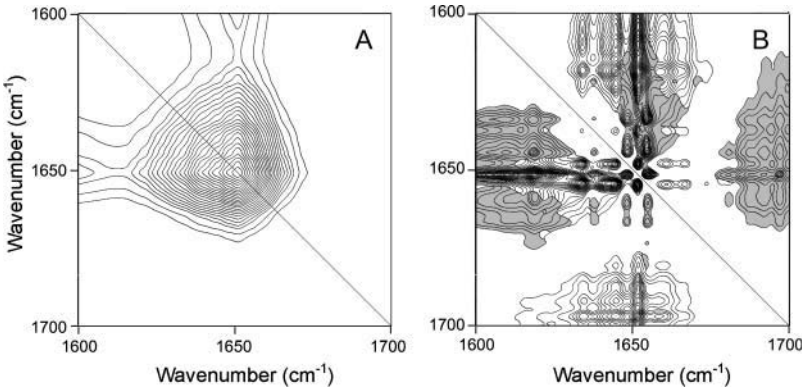

FIGURE 4 Two-dimensional correlation analysis of the IR spectra of Hb at the thermal unfolding stage. Synchronous (*A*) and asynchronous (*B*) plots were constructed from the six spectra recorded at temperatures increasing from 44 to 54°C. Clear and dark peaks are positive and negative, respectively.

the unfolding of α-helix is the major process in this temperature interval, which was consisted with the result in Fig. 1. Complex crosspeaks were found in the asynchronous plot (Fig. 4 *B*). The major secondary structure elements that could be characterized were α-helix (1652 and 1655 cm^{-1}), random coil (1644 and 1648 cm^{-1}), hydrogen-bonded extended chains that connect the helical cylinders (1634 and 1638 cm^{-1}), and β-turns (1674 and 1692 cm^{-1}). The new band at 1661 and 1666 cm^{-1} could be assigned to 3_{10}-helix, β-turn, or random coil (Dong et al., 2000; Jackson, 1989). Since 3_{10}-helix is a common structure in Hb, this band was assigned to native 3_{10}-helix in this work. The significant bands appearing near 1618 and 1681 cm^{-1} were assigned to side chain and β-turn at the initiate perturbation stage (30–44°C), and they were assigned to intermolecular β-sheet in this temperature interval since significant unfolding had already occurred (for details about the assignment, see the Discussion). The wavenumbers related to α-helix (1652 and 1655 cm^{-1}) structures were red-shifted when compared to those in Fig. 3 *B* (1653 and 1657 cm^{-1}), which suggested that the α-helix structures were more solvent-exposed in the unfolding stage. A closer inspection of the sign of the crosspeaks in the asynchronous plot suggested that two major classes of peaks could be distinguished in this temperature interval. The first class (tentatively called class I) was related to intensities at 1634, 1644, 1652, 1661, 1666, and 1674 cm^{-1}, which were before all other secondary structures correlated. The second class (class II) was related to intensities at 1638, 1648, and 1655 cm^{-1}, which were after all the secondary structures correlated. The changes of structures related to class I were earlier than those related to class II, and no correlated asynchronous crosspeak could be found among the same class. The change of the intermolecular β-sheet was after the changes of the class I structures. The order of sequential events during this temperature range are summarized here: extended chains (1634 cm^{-1}), random coil (1644 cm^{-1}), α-helix (1652 cm^{-1}), 3_{10}-helix (1661 and 1666 cm^{-1}), β-turns (1674 cm^{-1}) $\rightarrow$ extended chains (1638 cm^{-1}), random coil (1648 cm^{-1}), α-helix (1655 cm^{-1}), and intermolecular β-sheet (1618 and 1681 cm^{-1}).

Thermal aggregation of Hb from 54 to 70°C

The protein was at the thermal aggregation stage during the temperature interval from 54 to 70°C. The formation of aggregation, mentioned at the unfolding stage, could be identified more clearly during this temperature interval. During the temperature interval from 54 to 70°C, the dominant structure change of the protein was the unfolding of the native α-helix, as identified by the strong autopeaks at 1652 cm^{-1} in the synchronous plot (Fig. 5 *A*). The appearance of a strong negative crosspeak at 1616-1652 cm^{-1} in the synchronous plot indicated that the occurrence of protein aggregation, and the changes of α-helix and intermolecular β-sheet, had opposite directions (unfolding of the α-helix and formation of aggregation, respectively). In Fig. 5 *B*, positive asynchronous crosspeaks were found at 1652-1616 cm^{-1} and 1652-1682 cm^{-1}. An analysis of the sign of the crosspeaks appearing at the same wavenumber in the synchronous and asynchronous plots using the rules proposed by Noda (1990) suggested that the formation of aggregation was earlier than the unfolding of native α-helix, which is quite different from the conclusion made by constructed 2D IR correlation from whole temperature range (Fig. 2). Such a difference suggested that the formation of aggregation might arise from the structures already unfolded at the unfolding stage (44–54°C).

DISCUSSIONS

Protein thermal aggregation involves distinct regions

It is of usual interest to characterize events and regions of protein that are directly related to aggregation. However, it is difficult for normal probes to achieve such a characterization. In recent years, structural characterization of protein fibrils has been successfully studied by electron microscopy, x-ray diffraction, and NMR (Lansbury et al., 1995; Sunde et al., 1997; Antzutkin et al., 2002; Balbach et al., 2002; Serag et al., 2002). Nevertheless, relatively little is known about the initial stages of this process in solution. Generally, thermal

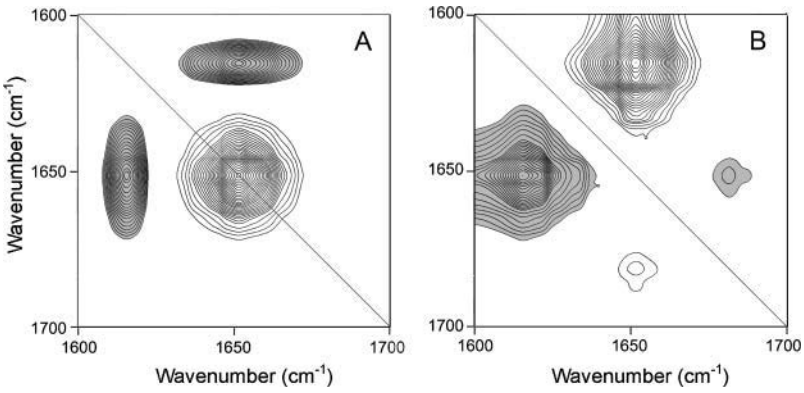

FIGURE 5 Two-dimensional correlation analysis of the IR spectra of Hb at the thermal unfolding stage. Synchronous (*A*) and asynchronous (*B*) plots were constructed from the nine spectra recorded at temperatures increasing from 54 to 70°C. Clear and dark peaks are positive and negative, respectively.

aggregation is associated with protein unfolding, which allows hydrophobic parts of different proteins to form intermolecular structures. However, the relationship of unfolding and aggregation is still a puzzle. Aggregation was also found to occur between nearly native proteins under certain conditions (Tsai et al., 1998; Paquet et al., 2001; Yan et al., 2003) and computer simulations (Smith and Hall, 2001). It is imaginable that the start of aggregates formation might not require fully unfolded proteins, but rather some necessary regions for the formation of intermolecular interactions. Such a hypothesis was supported by a close inspection of the data in this study.

The splitting of the helical absorption of Hb has been attributed to different hydrogen-bonding strengths. Since hydrogen bonding of the peptide carbonyl red-shifts the amide I absorption (Jackson et al., 1989), a lower wavenumber position is correlated with stronger hydrogen bonding and is more solvent-exposed than those at higher frequencies. The splitting of the helical absorption of Hb should be attributed to different solvent-exposed regions, whereas the low-frequency helices (1652 or 1653 cm^{-1} in Figs. 3 *B* or 4 *B*, respectively) have increased solvent exposure, yielding helices that are less stable than the more buried helices (1657 or 1655 cm^{-1} in Figs. 3 *B* or 4 *B*, respectively) at high-frequency. The different stability of these two components was supported by the observation of a strong negative crosspeak formed between 1655 and 1652 cm^{-1} in Fig. 4 *B*, which suggested that changes of the buried helical structures at 1655 cm^{-1} were after the more exposed helical structures at 1652 cm^{-1}. The red shift of the α-helix absorption at the unfolding stage when compared to the initiate perturbation stage was also related to the increased solvent exposure, suggesting a looser tertiary structure found at the unfolding stage.

The two distinct classes of intensities appearing in Fig. 4 *B* indicated that two processes existed during the first stage of Hb thermal transition. The first process was related to protein aggregation, which was identified by the correlated crosspeaks observed between bands that were characteristic of aggregation (1616 and 1681 cm^{-1}) and class I bands from native structures (1634 and 1652 cm^{-1}). The second process was related to further unfolding of class II regular structures (1638 and 1655 cm^{-1}), which was after the first process, and no crosspeaks could be observed correlated to aggregation. The changes of the class I intensities might be the origin of aggregation, whereas the class II was not. The existence of two classes of intensities in Fig. 4 *B* could also be distinguished in physiological temperatures (Fig. 3 *B*, represented by intensities at 1653 and 1657 cm^{-1}). There are no crosspeaks found in the asynchronous plot among the band in the same class, suggesting that events related to the same class were synchronous or cooperative. The different sequence between the unfolding of native structures and formation of aggregates found in Figs. 2 and 5 also indicated that the start of aggregation was from the structures already unfolded at the unfolding stage. These results give direct evidence to the hypothesis that thermal aggregation is related to a distinct region in the protein. This distinct region was more solvent-exposed and less stable.

The existence of such an aggregation nucleus has been observed in amyloid fibrillation by data from kinetic studies (Adachi and Asakura, 1980), NMR (Alexandrescu and Rathgeb-Szabo, 1999), mutational analysis (Chiti et al., 2002), or limited proteolysis (Azuaga et al., 2002). This was the first time it could be characterized that protein thermal aggregation also involves distinct region. This hypothesis could explain why thermal aggregation could start between nearly native proteins. Combining analysis of the results in Figs. 1 and 4 *B* also suggested that aggregation is rather a competing process than a driving force in protein thermal unfolding. Thus it could be concluded that aggregates might reserve a number of native structures when aggregates formed between native or partially folded proteins, as observed by several studies (Alexandrescu and Rathgeb-Szabo, 1999; Vermeer and Norde, 2000; Tobler and Fernandez, 2002).

Evolution of Hb thermal unfolding and aggregation

Distinct synchronous and asynchronous plots were found when the 2D IR correlation was constructed at each separate stage, as shown in Figs. 3–5. The lack of similarity made it difficult to correlate the different changes at each stage during Hb thermal transitions. To solve this problem, 2D IR plots were constructed at every 10°C intervals with a 2°C increase between every two plots. The synchronous plots were similar to Figs. 3 *A*, 4 *A*, or 5 *A* (plots not shown), which reflect that the main process was dominated by the changes of α-helix and extended chain structures below 44°C, the changes of α-helix between 46°C and 60°C, and the changes of α-helix and intermolecular β-sheet above 62°C. The change of the wavenumber of the amide I band from helical structure in the synchronous plot is presented in Fig. 6. A fast red shift was observed as temperature increased from 38 to 50°C, which suggested that the helical structures undergoing unfolding were more and more solvent-exposed as temperature increased. Of particular interest is that the band from α-helix moved to higher frequency at temperatures above 50°C, which suggested that the helical structures unfolding at a temperature above 50°C were less solvent-exposed. Comparison of Figs. 1 *B* and 6 indicated that this blue shift was at the thermal aggregation stage and accompanied by the formation of aggregates. This observation could also be explained by the hypothesis of distinct regions involved in protein thermal aggregation. The tertiary structure of Hb became more and more loose when suffered to heat denaturation at the unfolding stage. The highly solvent-exposed region unfolded first and was the origin of aggregates. The buried region still maintained the regular structure

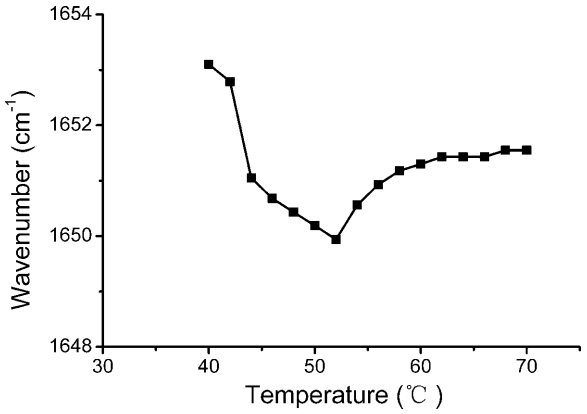

FIGURE 6 Frequency change at the major helical autopeak in the synchronous plots as a function of temperature for Hb thermal transition. The synchronous 2D IR correlation plots were constructed at every 10°C intervals with 2°C increase between two adjacent plots from spectra recorded at temperatures increasing from 30 to 70°C. The frequency of the autopeak at each plot was represented by the end temperature at the corresponding interval.

in aggregates and underwent a further unfolding at the aggregation stage.

Different out-of-phase events were found to dominate different temperature intervals, as shown in Fig. 7 (only selected plots are shown for clarity). Such a difference suggested that though a simple two-state or three-state model was used to illustrate the thermal transition of proteins, significant noncooperative events might occur at the transition states. These noncooperative events reveal different local thermal stabilities of the protein. This was also observed in the thermal unfolding process of myoglobin (Yan et al., 2003). Both theoretical and experimental studies have provided valuable information on the different local stabilities of proteins (Muthusamy et al., 2000; Matheson and Scheraga, 1979). Probing such noncooperative events might help us to find the origin of protein unfolding and aggregation, which in turn would facilitate the developing of enhancing protein thermal stability and avoiding uncontrolled aggregation. It should be noted that the asynchronous 2D IR plot only reflects the noncooperative events occurring upon perturbation. These noncooperative events might not be the predominant events during transition (as those reflected by the synchronous plot).

For purpose of illustration, a scheme that considers the transition state as composed of an ensemble of microstates was proposed to explain how these noncooperative events occur along with the predominant events. The native states N_1 and N_2 reflect different transition states at the initial structural perturbation stage. Each native transition state comprises an ensemble of microstates, which are denoted by different lower-case letters in Scheme I. Neighboring letters in the alphabet indicate microstates with similar conformations. For example, N_1 comprises *a*, *b*, and *c* microstates, with *a* being the most compact species, *c* being the least compact, and *b* being the predominant species. At the initial perturbation stage, though little perturbation of the native structure was observed, noncooperative events will be

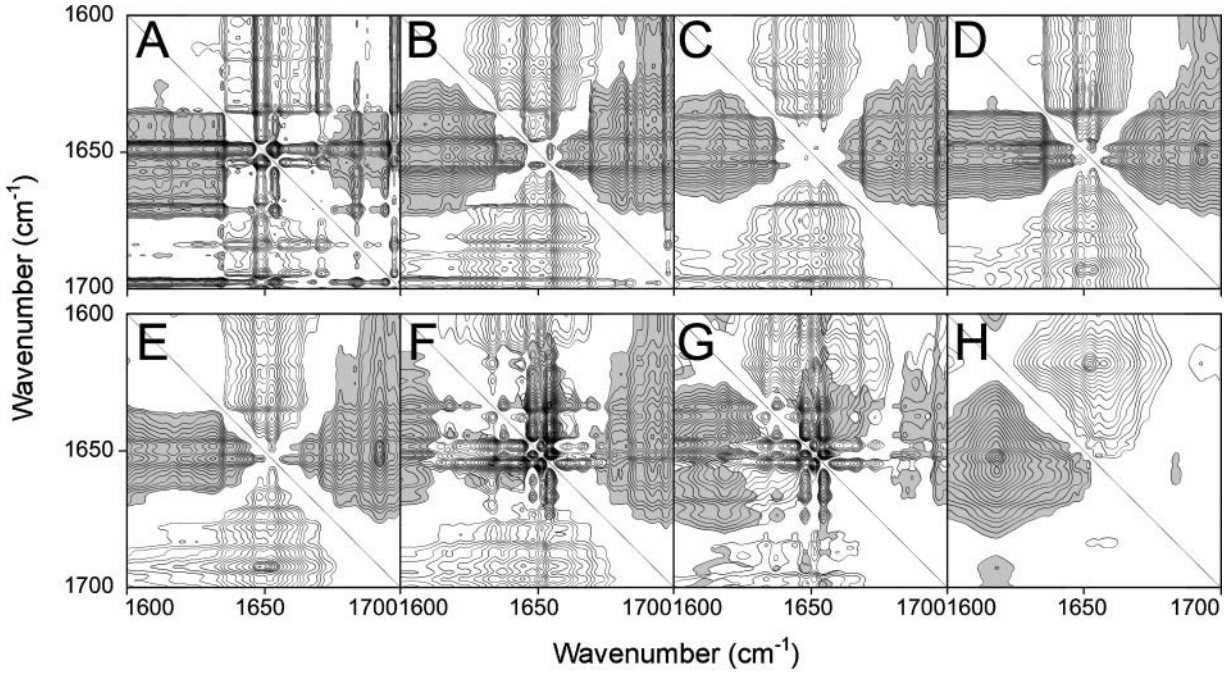

FIGURE 7 Evolution of the 2D IR asynchronous correlation plots. The synchronous plots were constructed in temperature ranges from 34 to 42°C (*A*), 36 to 44°C (*B*), 38 to 46°C (*C*), 40 to 48°C (*D*), 42 to 50°C (*E*), 44 to 52°C (*F*), 46 to 54°C (*G*), and 48 to 56°C (*H*). Clear and dark peaks are positive and negative, respectively.

$$N_1(a,b,c) \leftrightarrow N_2(a^*,b^*,c^*) \leftarrow\!-\!-\!-\!-\!-\!-\!\rightarrow U_1(l,m,n) \leftarrow\!-\!-\!-\!-\!-\!-\!\rightarrow U_n(o,p,q,x^*) -\!-\!-\!-\!-\!\rightarrow D(x,y,z)$$

SCHEME I

observed if the transition states (represented by N_1 and N_2 in Scheme I) have a different ensemble of microstates (Figs. 3 and 7 *A*). The asterisks in N_2 state reflect the slightly different microstates. At the start of the thermal unfolding stage, relatively few noncooperative events could be found (Fig. 7, *B–E*), whereas at the end of the thermal unfolding stage, more noncooperative events could be observed due to the formation of new structures (Fig. 7, *F* and *G*). This was demonstrated as the U_n state in Scheme I. The appearance of microstate x^* indicated the appearance of the newly formed intermolecular structures, whereas o, p, and q represented the different microstates from the start of the unfolding stage. At the thermal aggregation stage, the fast formation of the newly formed aggregates dominates the transition, and the major noncooperative event was related to aggregation. In Fig. 7 *H*, the appearance of the crosspeaks at 1657-1616 and 1657-1684 cm^{-1} suggested a further unfolding of the buried helical structures in aggregates. The new band located at 1698 cm^{-1} should be assigned to the C=O stretching mode of hydrogen-bonded COOH groups of Glu and Asp acid residues and aromatic amino acid residues (Barth, 2000; Murayama et al., 2001). The negative crosspeak at 1616-1698 cm^{-1} suggested that the formation of the intermolecular β-sheet structures came after the change of the hydrogen-bonded COOH groups. These noncooperative events could also be observed at higher temperature intervals. These results revealed that though the predominant changes could be demonstrated by a two-state or three-state model, protein thermal transition contains many noncooperative events that might be important to the start of aggregation. A careful 2D IR analysis might correlate these events and characterize the sequence of different events and thus has potential to provide distinct information on the mechanism and pathway(s) of thermal aggregation.

CONCLUSIONS AND PERSPECTIVES

The results obtained in this study indicated that IR spectroscopic investigations of protein thermal denaturation using a combination of 1D and 2D correlation analysis could provide novel and important information on the mechanism and pathway(s) of protein thermal aggregation. It is also noteworthy that all native secondary structure elements could be identified in the 2D IR correlation plots generated from spectra recorded under subtle perturbations at physiological conditions (Fig. 3). The ability of 2D IR correlation spectroscopy to monitor the minor structural changes might provide a potential powerful tool to characterize the native secondary structure elements in proteins (Y.-B. Yan and Q. Wang, unpublished data). This study revealed that Hb denatured by a two-stage thermal transition. At the initial perturbation stage (30–44°C), the change of random coil is earlier than all other secondary structure elements. As a result, the tertiary structure of the protein became looser and some of the native helical structures became more and more solvent-exposed indicated by the fast red shift of the band form α-helix as temperature increased. At the thermal unfolding stage, the unfolding of solvent-exposed helical structures dominated the transition. The solvent-exposed structures were supposed to be responsible for the start of aggregation. At the thermal aggregation stage, the transition was dominated by the formation of aggregates and the unfolding of the buried structures. A close inspection of the sequential events occurring at different stages suggested that protein thermal aggregation involves distinct regions. Sickle-cell disease arises from the polymerization of sickle-cell hemoglobin (HbS) at low oxygen concentrations. It has been found that normal hemoglobin and HbS aggregate by a similar mechanism (Adachi and Asakura, 1980). The results here might also be valuable to HbS studies. However, more investigations, using different methods besides 2D IR correlation spectroscopy applied to various proteins, are required to verify the hypothesis here and to characterize the regions directly related to aggregation.

The authors thank Dr. Q. Wu, Mrs. F. Liu, and Professor R.-Q. Zhang from Tsinghua University for stimulating discussions.

This investigation was supported by the Basic Research Funds of Tsinghua University, People's Republic of China, No. JC2002047; the 985 Funds of Tsinghua University, People's Republic of China; and funds from State Key Laboratory of Biomembrane and Membrane Biotechnology, People's Republic of China.

REFERENCES

Adachi, K., and T. Asakura. 1980. Aggregation and crystallization of hemoglobins A, S, and C. Probable formation of different nuclei for gelation and crystallization. *J. Biol. Chem.* 256:1824–1830.

Alexandrescu, A. T., and K. Rathgeb-Szabo. 1999. An NMR investigation of solution aggregation reactions preceding the misassembly of acid-denatured cold shock protein A into fibrils. *J. Mol. Biol.* 291:1191–1206.

Antzutkin, O. N., R. D. Leapman, J. J. Balbach, and R. Tycko. 2002. Supramolecular structural constraints on Alzheimer's β-amyloid fibrils from electron microscopy and solid-state nuclear magnetic resonance. *Biochemistry.* 41:15436–15450.

Azuaga, A. I., C. M. Dobson, P. L. Mateo, and F. Conejero-Lara. 2002. Unfolding and aggregation during the thermal denaturation of streptokinase. *Eur. J. Biochem.* 269:4121–4133.

Balbach, J. J., A. T. Petkova, N. A. Oyler, O. N. Antzutkin, D. J. Gordon, S. C. Meredith, and R. Tycko. 2002. Supramolecular structure in full-length Alzheimer's β-amyloid fibrils: evidence for a parallel β-sheet organization from solid-state nuclear magnetic resonance. *Biophys. J.* 83:1205–1216.

Barth, A. 2000. The infrared absorption of amino acid side chains. *Prog. Biophys. Mol. Biol.* 74:141–173.

Bulone, D., V. Martorana, and P. L. San Biagio. 2001. Effects of intermediates on aggregation of native bovine serum albumin. *Biophys. Chem.* 91:61–69.

Byler, D. M., and H. Susi. 1986. Examination of the secondary structure of proteins by deconvolved FTIR spectra. *Biopolymers.* 25:469–487.

Carrell, R. W., and B. Gooptut. 1998. Conformational changes and disease—serpins, prions and Alzheimer's. *Curr. Opin. Struct. Biol.* 8:799–809.

Carrotta, R., R. Bauer, R. Waninge, and C. Rischel. 2001. Conformational characterization of oligomeric intermediates and aggregates in β-lactoglobulin heat aggregation. *Protein Sci.* 10:1312–1318.

Chiti, F., N. Taddei, F. Baroni, C. Capanni, M. Stefani, G. Ramponi, and C. M. Dobson. 2002. Kinetic partitioning of protein folding and aggregation. *Nat. Struct. Biol.* 9:137–143.

Damaschun, G., H. Damaschun, H. Fabian, K. Gast, R. Kröber, M. Wieske, and D. Zirwer. 2000. Conversion of yeast phosphoglycerate kinase into amyloid-like structure. *Proteins.* 39:204–211.

Dong, A., and W. S. Caughey. 1994. Infrared methods for study of hemoglobin reactions and structures. *Methods Enzymol.* 232:139–175.

Dong, A., P. Huang, and W. S. Caughey. 1990. Protein secondary structure in water from second-derivative amide I infrared spectra. *Biochemistry.* 29:3303–3308.

Dong, A., T. W. Randolph, and J. F. Carpenter. 2000. Entrapping intermediates of thermal aggregation in α-helical proteins with low concentration of guanidine hydrochloride. *J. Biol. Chem.* 275:27689–27693.

Fabian, H., H. H. Mantsch, and C. P. Schultz. 1999. Two-dimensional IR correlation spectroscopy: sequential events in the unfolding process of the λ Cro-V55C repressor protein. *Proc. Natl. Acad. Sci. USA.* 96:13153–13158.

Filosa, A., Y. Wang, A. A. Ismail, and A. M. English. 2001. Two-dimensional infrared correlation spectroscopy as a probe of sequential events in the thermal unfolding of cytochromes c. *Biochemistry.* 40:8256–8263.

Haris, P. I., and D. Chapman. 1995. The conformational analysis of peptides using Fourier transform IR spectroscopy. *Biopolymers.* 37: 251–263.

Hoffner, G., and P. Djian. 2002. Protein aggregation in Huntington's disease. *Biochimie.* 84:273–278.

Jackson, M., P. I. Haris, and D. Chapman. 1989. Fourier transform infrared spectroscopic studies of lipids, polypeptides and proteins. *J. Mol. Struct.* 214:329–355.

Kopito, R. R. 2000. Aggresomes, inclusion bodies and protein aggregation. *Trends Cell Biol.* 10:524–530.

Lansbury, P. T., P. R. Costa, J. M. Griffiths, E. J. Simon, M. Auger, K. J. Halverson, D. A. Kocisko, Z. S. Hendsch, T. T. Ashburn, R. G. S. Spencer, B. Tidor, and R. G. Griffin. 1995. Structural model for the β-amyloid fibril based on interstrand alignment of an antiparallel-sheet comprising a C-terminal peptide. *Nat. Struct. Biol.* 2:990–998.

Lumry, R., and H. Eyring. 1954. Conformational changes of proteins. *J. Phys. Chem.* 58:110–120.

Lyubarev, A. E., B. I. Kurganov, V. N. Orlov, and H.-M. Zhou. 1999. Two-state irreversible thermal denaturation of muscle creatine kinase. *Biophys. Chem.* 79:199–204.

Matheson, R. R., and H. A. Scheraga. 1979. Steps in the pathway of the thermal unfolding of ribonuclease A. A nonspecific photochemical surface-labeling study. *Biochemistry.* 18:2437–2445.

Murayama, K., Y. Wu, B. Czarnik-Matusewicz, and Y. Ozaki. 2001. Two-dimensional/attenuated total reflection infrared correlation spectroscopy studies on secondary structural changes in human serum albumin in aqueous solutions: pH-dependent structural changes in the secondary structures and in the hydrogen bonding of side chains. *J. Phys. Chem. B.* 105:4763–4769.

Muthusamy, R., M. M. Gromiha, and P. K. Ponnuswamy. 2000. On the thermal unfolding character of globular proteins. *J. Protein Chem.* 19: 1–8.

Nabet, A., and M. Pézolet. 1997. Two-dimensional FT-IR spectroscopy: A powerful method to study the secondary structure of proteins using H-D exchange. *Appl. Spectrosc.* 51:466–469.

Noda, I. 1989. Two-dimensional infrared spectroscopy. *J. Am. Chem. Soc.* 111:8116–8118.

Noda, I. 1990. Two-dimensional infrared (2D-IR) spectroscopy: theory and applications. *Appl. Spectrosc.* 44:550–561.

Noda, I. 1993. Generalized two-dimensional correlation method applications to infrared, Raman, and other types of spectroscopy. *Appl. Spectrosc.* 47:1329–1336.

Noguchi, C. T., and A. N. Schechter. 1985. Sickle hemoglobin polymerization in solution and in cells. *Annu. Rev. Biophys. Biophys. Chem.* 14:239–263.

Paquet, M.-J., M. Laviolette, M. Pézolet, and M. Auger. 2001. Two-dimensional infrared correlation spectroscopy study of the aggregation of cytochrome c in the presence of dimyristoylphosphatidylglycerol. *Biophys. J.* 81:305–312.

Schreiber, G. 2002. Kinetic studies of protein-protein interactions. *Curr. Opin. Struct. Biol.* 12:41–47.

Schultz, C. P., H. Fabian, and H. H. Mantsch. 1998. Two-dimensional mid-IR and near-IR correlation spectra of ribonuclease A: using overtones and combination modes to monitor changes in secondary structure. *Biospectroscopy.* 4:S19–S29.

Serag, A. A., C. Altenbach, M. Gingery, W. L. Hubbell, and T. O. Yeates. 2002. Arrangement of subunits and ordering of β-strands in an amyloid sheet. *Nat. Struct. Biol.* 9:734–739.

Smith, A. V., and C. K. Hall. 2001. Protein refolding versus aggregation: computer simulations on an intermediate-resolution protein model. *J. Mol. Biol.* 312:187–202.

Srisailam, S., T. Krishnaswamy, T. K. S. Kumar, D. Rajalingam, K. M. Kathir, H. S. Sheu, F. J. Jan, P. C. Chao, and C. Yu. 2003. Amyloid-like fibril formation in an all β-barrel protein. Partially structured intermediate state(s) is a precursor for fibril formation. *J. Biol. Chem.* 278:17701–17709.

Sunde, M., L. C. Serpell, M. Bartlam, P. E. Fraser, M. B. Pepys, and C. C. F. Blake. 1997. Common core structure of amyloid fibrils by synchrotron x-ray diffraction. *J. Mol. Biol.* 273:729–739.

Thirumalai, D., D. K. Klimov, and R. I. Dima. 2003. Emerging ideas on the molecular basis of protein and peptide aggregation. *Curr. Opin. Struct. Biol.* 13:146–159.

Tobler, S. A., and E. J. Fernandez. 2002. Structural features of interferon-gamma aggregation revealed by hydrogen exchange. *Protein Sci.* 11:1340–1352.

Tsai, A. M., J. H. van Zanten, and M. J. Betenbaugh. 1998. Study of protein aggregation due to heat denaturation: a structural approach using circular dichroism spectroscopy, nuclear magnetic resonance, and static light scattering. *Biotechnol. Bioeng.* 59:273–280.

Vermeer, A. W. P., and W. Norde. 2000. The thermal stability of immunoglobulin: unfolding and aggregation of a multi-domain protein. *Biophys. J.* 78:394–404.

Yan, Y.-B., Q. Wang, H.-W. He, X.-Y. Hu, R.-Q. Zhang, and H.-M. Zhou. 2003. Two-dimensional infrared correlation spectroscopy study of sequential events in the heat-induced unfolding and aggregation process of myoglobin. *Biophys. J.* 85:1959–1967.

Yan, Y.-B., R.-Q. Zhang, and H.-M. Zhou. 2002. Biphasic reductive unfolding of ribonuclease A is temperature dependent. *Eur. J. Biochem.* 269:5314–5322.